

Microwave and mechanical properties of quartz/graphene-based polymer nanocomposites

B. J. P. Adohi, D. Bychanok, B. Haidar, and C. Brosseau

Citation: *Appl. Phys. Lett.* **102**, 072903 (2013); doi: 10.1063/1.4793411

View online: <https://doi.org/10.1063/1.4793411>

View Table of Contents: <http://aip.scitation.org/toc/apl/102/7>

Published by the [American Institute of Physics](#)

Articles you may be interested in

[A review and analysis of microwave absorption in polymer composites filled with carbonaceous particles](#)

Journal of Applied Physics **111**, 061301 (2012); 10.1063/1.3688435

[Measurement of the microwave effective permittivity in tensile-strained polyvinylidene difluoride trifluoroethylene filled with graphene](#)

Applied Physics Letters **104**, 082902 (2014); 10.1063/1.4866419

[The electromagnetic property of chemically reduced graphene oxide and its application as microwave absorbing material](#)

Applied Physics Letters **98**, 072906 (2011); 10.1063/1.3555436

[Microwave absorption properties of the carbon-coated nickel nanocapsules](#)

Applied Physics Letters **89**, 053115 (2006); 10.1063/1.2236965

[A comparison between physical properties of carbon black-polymer and carbon nanotubes-polymer composites](#)

Journal of Applied Physics **108**, 074108 (2010); 10.1063/1.3486491

[Exchange resonance modes in a ferromagnetic sphere](#)

Journal of Applied Physics **69**, 7762 (1991); 10.1063/1.347502

PHYSICS TODAY

WHITEPAPERS

MANAGER'S GUIDE

Accelerate R&D with
Multiphysics Simulation

READ NOW

PRESENTED BY

 COMSOL

Microwave and mechanical properties of quartz/graphene-based polymer nanocomposites

B. J. P. Adohi,^{1,2} D. Bychanok,^{1,3} B. Haidar,⁴ and C. Brosseau^{1,a)}

¹Université Européenne de Bretagne, Lab-STICC, Université de Brest, CS 93837, 6 avenue Le Gorgeu, 29238 Brest Cedex 3, France

²Laboratoire de Physique de l'Atmosphère et de Mécanique des Fluides, UFR-SSMT, Université Félix Houphouët-Boigny de Cocody, 22 BP 582 Abidjan 22, Ivory Coast

³Research Institute for Nuclear Problems, Belarus State University, Bobruiskaya str. 11, 220030 Minsk, Belarus

⁴Institut de Science des Matériaux de Mulhouse (IS2M), 15, rue Jean Starcky, BP 2488, 68057 Mulhouse Cedex, France

(Received 19 January 2013; accepted 11 February 2013; published online 20 February 2013)

We report microwave spectroscopy studies of graphene-based polymer-matrix composite materials subject to uniaxial elongation. The samples were prepared via shear mixing under the same thermal processing conditions of amorphous styrene butadiene rubber (SBR) with quartz grains on the order of micrometers in size and/or graphene sheets with thickness 10–20 nm and average lateral size 200 μm . An important result is the observation of a significant increase (up to 25%) in the effective microwave permittivity of hybridized nanocomposites comprising both quartz and graphene compared to the nanocomposites with quartz only. We suggest that the coating of quartz grains by graphene sheets is the most likely origin of this synergetic effect. In all cases, we also observe that the permittivity spectrum is unaffected by strain up to 8%. By examining the mechanical response, it is shown that the elasticity network of SBR polymer chains is significantly affected in the rubbery state by filling SBR with graphene and quartz particles. © 2013 American Institute of Physics. [<http://dx.doi.org/10.1063/1.4793411>]

The past two decades have witnessed a rapid increase in the design and fabrication of multifunctional materials appropriate for the next generation of plastic electronic devices which require reduced feature sizes, enhanced operating speeds, and low consumption. For recent reviews on the subject, we refer the reader to Refs. 1 and 2. Research on this area has been driven by rapid developments of quantitative computational models that have made possible the design and manipulation of multifunctional heterostructures,³ and experimental approaches in the fabrication of nanoparticle-polymer composite materials.^{4–6} Among the many structures of interest, several groups have focused on the physical and physicochemical properties of graphene filled polymers.^{7–16} These soft polymer-based nanostructures have emerged as attractive materials for studying energy storage, touch screens, actuators, and sensors, to name but a few. While these studies have unveiled advanced applications, they have not addressed the study of microwave properties of these materials under uniaxial extension which can be relevant for designing nano-electromechanical systems.

Recognizing the effects of mixing solid particles in elastic polymer matrix, several piezorheological and magnetorheological studies have been carried out.¹⁷ The relevance of possible coupling interactions between piezoelectric grains serving as transducer and conducting particles for charge carrier dissipation in polymer hosts has been also a topic of debate.^{4,18} Identification of the specific structural and electric characteristics that drive the emergence of electromechanical coupling in these polymeric materials is a central experimental and

theoretical question in the field. Microwave spectroscopy studies that probe the variation of permittivity as a function of filler content are lacking but are desirable to understand the nature of these electromechanical couplings. Additionally, many reports have described the elasticity network of filled polymers.¹⁸ The application of the volume-conserving uniaxial deformation can be modeled phenomenologically by assuming that the elasticity network in the material occurs in a manner that is topologically similar to the elasticity network of a conventional rubber, i.e., assuming purely affine entropic stretching deformations.^{18,19} Motivated by these results, we consider it highly desirable to characterize the effect of mechanical strain on the electromagnetic wave transport in multifunctional materials containing piezoelectric and conducting inclusions.

As discussed by Qin and Brosseau, a growing number of demanding applications in electronics and telecommunications rely on the unique properties of C allotropes.⁴ Nanographene sheets are being studied as elements in electronic devices since they host a two-dimensional electronic transport, have high heat conductivity, ultrahigh electron mobility, large surface area, high thermal conductivity, and possess also high thermal and mechanical stability.⁷ Recently, dispersion of electric charges have been demonstrated with graphene-based nanocomposites.²⁰ Microwave applications of graphene and graphene-based polymer composites remain largely unexplored. Utilizing graphene would be particularly attractive because of the possibility of implementing artificial two-dimensional structures in potential microwave devices.²¹ However, this issue continues to be challenging, in part, because of the impedance mismatch.⁷

^{a)}Email: brosseau@univ-brest.fr.

In this letter, we aim to experimentally investigate the effective permittivity of quartz/graphene-based polymer nanocomposites. Due to the large surface area of graphene, proximity effects are expected to occur at such piezoelectric/conducting interfaces. By comparing the values of the effective permittivity in different samples with or without quartz grains, we find a significant increase (up to 25%) in the effective microwave permittivity of samples containing quartz and graphene. This permittivity increase might arise from the coating of quartz grains by graphene sheets. The mechanical response of these filled polymers shows that there is significant change in their elasticity network above $T_g + 50^\circ\text{C}$.

Amorphous styrene butadiene rubber (SBR) supplied by Lanxess, Germany was used as the matrix. The styrene content is 23%. Dicumylperoxide was used as crosslinking agent. Large-area graphene sheets (obtained from Angstrom Materials Inc., USA) and/or α -quartz (purchased from Carl Roth) filled SBR composites were fabricated by conventional shear mixing. First, SBR was mixed with or without graphene and/or quartz in a Brabender mixer. Then, dicumylperoxide (0.5 phr) was added in a two-mill mixer. Finally, the compounds were placed in a 1.6 mm thick aluminium mold and cured at 160°C during 60 min. The average size of quartz grains is $50\ \mu\text{m}$. The grade N006-P graphene powder (C content $\approx 97\%$ and O content $\approx 1.5\%$) is constituted of a graphene sheets stacked together with thickness 10–20 nm and average lateral size $200\ \mu\text{m}$. Three sample sets (A, B, and C) with different amounts of graphene and quartz were fabricated. In series A, sample 1 is pure SBR, sample 2 is SBR with graphene content of 0.1 phr, sample 3 is SBR with quartz content of 10 phr, and sample 4 is SBR with graphene content of 0.1 phr and quartz content of 10 phr. Series B differ from series A by the quartz content which is set to 5 phr, and series C contains 1 phr of quartz. The morphology of the samples was characterized via scanning electron microscopy (SEM). For samples containing quartz, cross-sectional SEM analysis revealed a quasi-uniform distribution of quartz grains (not shown).

Room temperature microwave measurements of the scattering parameters (S parameters) were carried out using an Agilent H8753ES vector network analyzer with SOLT calibration. Each sample was mounted in an asymmetric microstrip transmission line. The test device is used as Thru in the transmission connection. Control of data acquisition and data storage is accomplished with LABVIEW 6.1 (National Instruments) graphical programming software operating in a Windows 2000 environment. The dielectric parameters of the samples are extracted via an explicit coarse-grained procedure to reduce the problem to a simpler one consisting of measuring the single effective complex permittivity $\varepsilon = \varepsilon_0(\varepsilon' - j\varepsilon'')$ of the material under test, where $\varepsilon_0 \approx 8.85 \times 10^{-12}\ \text{F m}^{-1}$ is the permittivity of free space. The experimental protocol of Ref. 18 determines the measurement of ε as function of the applied tensile force. The present results have a statistical error in ε' of about $\pm 3\%$ and in ε'' of about $\pm 2\%$. We assume the particle size to be small compared to the wavelength so that the skin effect is negligible. In the experiments reported here, the samples have dimensions $70\ \text{mm}$ [length] $\times 5\ \text{mm}$ [width] $\times 1.6\ \text{mm}$ [thickness]. The elongation ratio λ is defined as $\lambda = \ell/\ell_0$. Here, the length ℓ of the rectangular-shaped sample is measured with respect to

the length ℓ_0 the corresponding sample has initially. For these microwave measurements, samples containing quartz are unpoled. We also measured repeats of selected samples to confirm that obtained results are not just associated with a particular batch of samples.

To complement the current electromagnetic analysis, elastic properties of these hybrid polymer nanocomposites have been probed by dynamic mechanical analysis (DMA). The dynamic storage and loss moduli, E' and E'' , respectively, of the composite samples were examined by a DMA Metravib as function of temperature from -150 to 100°C at 10 Hz and sweeping from low to high temperature with a $2^\circ/\text{min}$ heating rate. The sample was checked to be within the linear viscoelastic regime where E' and E'' are independent of the applied stress. Samples used for DMA are prepared as rectangular parallelepipeds of $1\ \text{mm}$ [thickness] $\times 10\ \text{mm}$ [width] $\times 20\ \text{mm}$ [length].

Our primary results are contained in Fig. 1 which shows one set of relative variation of the (real part) effective permittivity spectra normalized with respect to sample A1 at two elongation ratios ($\lambda = 1$ corresponding to the unstrained sample, and $\lambda = 1.02$). These spectra are flat over the frequency range investigated. Interestingly, no appreciable differences between the permittivity of the strained and unstrained samples are seen in Fig. 1. This feature remains valid for all samples investigated. From this comparison, we conclude that there is a significant ε' enhancement of the sample comprising both quartz and graphene (up to 25%) compared to the nanocomposites with quartz only. This is not a piezoelectric response as is the case for many quartz-based composites. The mechanism responsible for these unanticipated observations is not yet confirmed; however, we propose that some nanoscale contact areas between graphene sheets and quartz grains exist. Since the quartz content is low and the filler particles are quasi-uniformly dispersed and randomly oriented within the composite samples, quartz

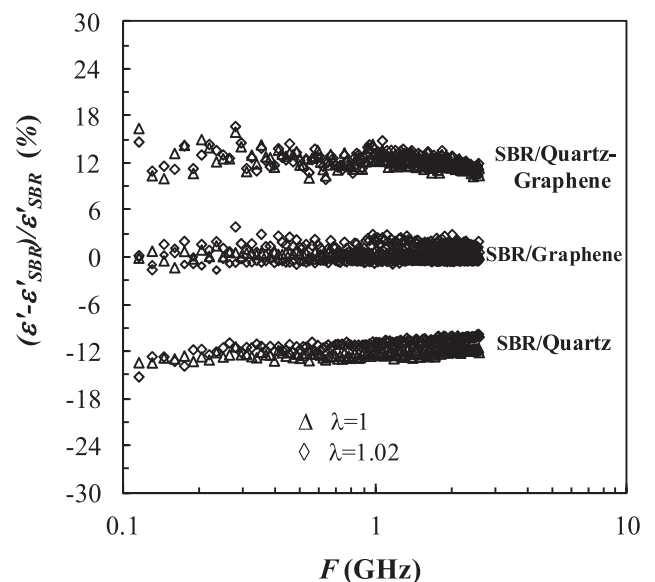


FIG. 1. Relative variation of the real part of the effective permittivity ε' , normalized to that of sample A1 (neat SBR), as a function of frequency for samples A2 (SBR/graphene), A3 (SBR/quartz), and A4 (SBR/quartz-graphene) and two values of the elongation ratio λ : (triangles) $\lambda = 1$, (diamonds) $\lambda = 1.02$ (room temperature).

particles are disconnected from each other and the conductance is mediated by a quantum intertunneling mechanism between these particles (nonpercolative transport regime). We consider that the tunnelling mechanism is dominated by quartz because it is the main filler phase. We suggest that graphene-wrapping of the quartz grains is the mechanism for the observed permittivity increase shown in Fig. 1. In this context, the filler particles in our sample can be considered as graphene-coated quartz particles with a nano-scale coating thickness. Several studies have addressed the dielectric properties of core-shell (CS) composites, e.g., see Ref. 22. Liu *et al.*²² have shown that CS spherical particles (formed by a core of permittivity ϵ_1 and radius a and a shell of permittivity ϵ_2 and thickness $b-a$, b being the radius of the overall CS particle) randomly dispersed in a host matrix (permittivity ϵ_m) are equivalent to homogeneous spherical particles with equivalent permittivity $\gamma\epsilon_1$ where $\gamma = [\beta(1+2\beta) + 2\alpha\beta(1-\beta)] / [(1+2\beta) - \alpha(1-\beta)]$ with $\beta = \epsilon_2/\epsilon_1$ and $\alpha = (a/b)^3$. A mathematical discussion of this model can be found in Ref. 22 under the assumption $\epsilon_2 > \epsilon_m$ (present case). For our purpose, two important facts are: (1) the effective permittivity of CS composites can increase significantly as a function of the shell volume fraction compared to the case of the core phase only, and (2) the effective permittivity has a maximum when the filler volume fraction is varied. It is not possible to compare our experimental results with these theoretical predictions, but the former are consistent with the latter. The values of ϵ'' are generally small (<0.1) and show a large amount of scatter (due to the analyzer's sensitivity). They will not be discussed in this work.

Furthermore, In Fig. 1, we show the relative variations of ϵ' content for the series A submitted to a uniaxial strain. We note that even though we are applying a small mechanical deformation the spectral profile of ϵ' remains flat in the frequency range explored. This is at variance with similar observations on a variety of filled polymers for which the monotonic increase of the relative permittivity change $(\epsilon'(\lambda=1) - \epsilon'(\lambda > 1)) / \epsilon'(\lambda=1)$ as a function of the extension ratio λ can be rationalized applying the Gaussian Molecular Network Model (GMNM) functional form $(\lambda - \lambda^{-2})$.¹⁸ Furthermore, since many fascinating predictions have been made regarding magnetism in graphene,²³ we also attempted permittivity measurement under a magnetic field up to 2 kG on unstrained samples of series A. However, the experiment was inconclusive and no signature of magneto-electric behavior was observed. The analysis of the length, width, and thickness normalized to their initial value, examined as a function of λ display interesting trends: the two perpendicular directions experience (not shown) the symmetric contraction by $1/\sqrt{\lambda}$ and the principal direction is elongated by λ . From this, we can infer that these variations reflect volume conservation of the elasticity network. In other words, it confirms that the Poisson ratio is ≈ 0.5 . Since we could measure the permittivity under stress up to 8%, a good stretchability is obtained, which is also an indication of good adhesion between filler particles and SBR.

To further investigate the connection of permittivity to filler particles mesostructure, we studied the spectral evolution of ϵ' with quartz content for series A, B, and C of samples. Our measurements (not shown) indicate that the

hierarchy in the relative variation of permittivity is quite similar to that displayed in Fig. 1. The effect of varying the quartz content on ϵ' (1 GHz) is shown in Fig. 2 for several values of graphene weight fractions and two elongation ratios. There is an optimal range for the permittivity increase with quartz content at round 5 phr since it decreases thereafter. In addition, comparison of the values of ϵ' (1 GHz) shows little change between unstrained and strained samples.

The mechanical response for the series A echoes the overall microwave response under strain, but contains some distinct features. Shown in Figs. 3(a) and 3(b) are curves of storage and loss moduli in the -150 – 100 °C range. These results do not indicate any simple dependence on graphene and quartz contents. We found that filling SBR with quartz and graphene has no effect on the glass transition temperature $T_g \approx -45$ °C. Only the rubbery plateau seems to be affected. We found that E' and E'' of graphene filled samples are significantly decreased above T_g . While the storage modulus of SBR is equal to 2.11 MPa at room temperature, it decreases significantly by 70% to 0.63 MPa when SBR contains 0.1 phr of graphene. However, this decrease is attenuated by the addition of quartz to the graphene filled samples and virtually vanishes when quartz is used alone, i.e., equal to 2.39 when SBR contains 10 phr of quartz. This is contrast to the standard observations of improvements in the mechanical properties of polymer matrices at very small loadings.^{4,24,25} However, several studies²⁴ reported a decrease of the modulus values in graphene filled polymer sample mainly caused by the defects produced either during graphite oxidation or graphite oxide thermal exfoliation and suggested that high aspect ratio graphene sheets once dispersed in a polymer adopt wrinkled structures which may effectively reduce moduli, as crumpled platelets tend to unfold rather than stretch in-plane under an applied tensile stress. This is further evidence that the filler particles

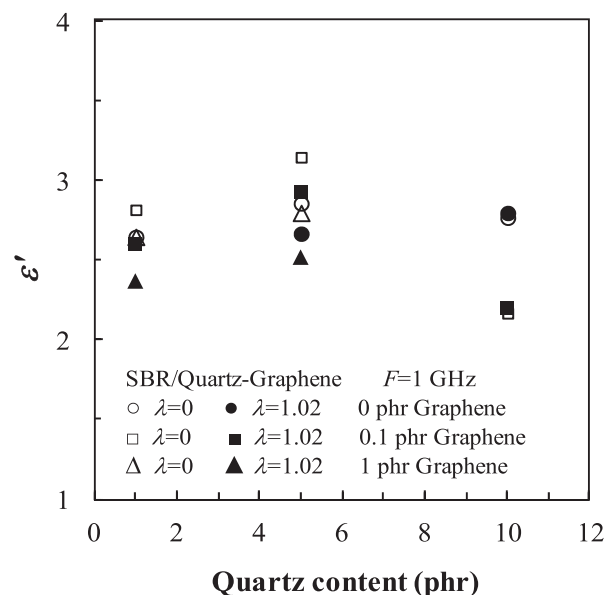


FIG. 2. A comparison between the values of ϵ' for series A, B, and C as a function of quartz content. Symbols are: (circles) 0 phr graphene, (squares) 0.1 phr graphene, and (triangles) 1 phr graphene. $F = 1$ GHz. Open symbols correspond to unstrained samples while filled symbols correspond to strained samples ($\lambda = 1.02$) (room temperature).

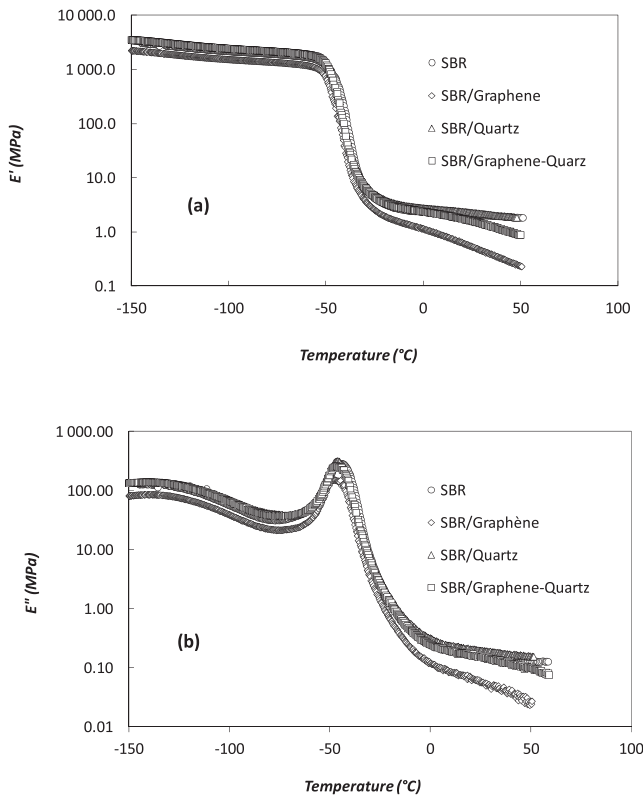


FIG. 3. (a) Storage modulus for samples of series A as a function of temperature. The symbols used in this figure are: (circles) SBR, (triangles) SBR/quartz, (diamonds) SBR/graphene, (squares) SBR/quartz-graphene. (b) Same as in (a) for the loss modulus.

mesostructure have a significant collective effect on the elasticity network of SBR polymer chains. It is also worth noting that a loss of the elastic properties for nanoparticle/polymer composites can be explained by the decrease in the blend density below the bulk polymer density level and the nature of the nanoparticle/polymer interactions.²⁶

To briefly conclude, our comparative study on the dielectric response of ternary hybrid systems composed of graphene and quartz filled SBR demonstrates that using low loadings of graphene these systems can have superior dielectric properties. Based on our experiments, we attribute the 25% increase in permittivity to the graphene coating of the quartz grains in the composite samples. In the low strain regime, we have also shown that the elasticity network of SBR polymer chains is significantly affected by filler particles addition above $T_g + 50^\circ\text{C}$. It is our hope that the unique features of these hybrid nanostructured composites with organic and inorganic filler particles could be exploited for engineering energy storage in future plastic microwave devices and lightweight shielding materials for microwave radiation.¹

We would like to thank G. Mignot for assistance with microwave measurements of the samples. B.J.P.A. is grateful for support from the Université de Brest, Lab-STICC (Unité Mixte de Recherche CNRS 6285), and IS2M (Unité Mixte de Recherche CNRS-UHA 7361).

¹C. Brosseau, *Surf. Coat. Technol.* **206**, 753 (2012).

²G. H. Gelinck, H. E. A. Huitema, E. van Veenendaal, E. Cantatore, L. Schrijnemakers, J. B. P. H. van der Putten, T. C. T. Geuns, M.

- Beenhakkers, J. B. Giesbers, B.-H. Huisman, E. J. Meijer, E. M. Benito, F. J. Touwslager, A. W. Marsman, B. J. E. van Rens, and D. M. de Leeuw, *Nature Mater.* **3**, 106 (2004).
- ³C. Brosseau, *Computational Electromagnetics: From the Design of Heterostructures to the Modeling of Biostructures* (unpublished).
- ⁴F. Qin and C. Brosseau, *J. Appl. Phys.* **111**, 061301 (2012).
- ⁵J. Lu and C. P. Wong, "Nanoparticle-based high-k dielectric composites: Opportunities and challenges," in *Nanopackaging: Nanotechnologies and Electronics Packaging*, edited by J. E. Morris (Springer, New York, 2008).
- ⁶C. Brosseau, P. Queffelec, and P. Talbot, *J. Appl. Phys.* **89**, 4532 (2001); C. Brosseau, J. Ben Youssef, P. Talbot, and A.-M. Konn, *ibid.* **91**, 3197 (2002); C. Brosseau, S. Mallécol, P. Queffelec, and J. Ben Youssef, *ibid.* **70**, 092401 (2004); S. Mallécol, C. Brosseau, P. Queffelec, and A.-M. Konn, *ibid.* **68**, 174422 (2003); J. Ben Youssef and C. Brosseau, *ibid.* **74**, 214413 (2006).
- ⁷K. S. Novoselov, A. K. Geim, S. V. Morozov, D. Jiang, Y. Zhang, S. V. Dubonos, I. V. Grigorieva, and A. Firsov, *Science* **306**, 666 (2004); A. K. Geim and K. S. Novoselov, *Nature Mater.* **6**, 183 (2007); S. Stankovich, D. A. Dikin, G. H. B. Dommett, K. M. Kohlhaas, E. J. Zimney, and E. A. Stach, *Nature* **442**, 282 (2006); J. Yan, Y. Zhang, P. Kim, and A. Pinczuk, *Phys. Rev. Lett.* **98**, 166802 (2007); G. Eda, G. Fanchini, and M. Chowalla, *Nat. Nanotechnol.* **3**, 270 (2008); J. T. Robinson, F. K. Perkins, E. S. Snow, Z. Q. Wei, and P. E. Shehan, *Nano Lett.* **8**, 3137 (2008); S. K. Pati, T. Enoki, and C. N. R. Rao, *Graphene and Its Fascinating Attributes* (World Scientific, Singapore, 2011); J. S. Bunch, A. M. van der Zande, S. S. Verbridge, I. W. Frank, D. M. Tanenbaum, J. M. Parpia, H. G. Craighead, and P. L. McEuen, *Science* **315**, 490 (2007); G. Deligeorgis, M. Dragoman, D. Neculoiu, D. Dragoman, G. Konstantinidis, A. Cismaru, and R. Plana, *Appl. Phys. Lett.* **95**, 073107 (2009); X. Huang, X. Y. Qi, F. Boey, and H. Zhang, *Chem. Soc. Rev.* **41**, 666 (2012).
- ⁸J. R. Potts, D. R. Dreyer, C. W. Bielawski, and R. S. Ruoff, *Polymer* **52**, 5 (2011).
- ⁹L. Cui, X. Lu, D. Chao, H. Liu, Y. Li, and C. Wang, *Phys. Status Solidi A* **208**, 459 (2011).
- ¹⁰V. E. Muradyan, E. A. Sokolov, N. P. Piven, S. D. Babenko, and S. R. Allayarov, *Tech. Phys. Lett.* **36**, 1115 (2010).
- ¹¹J. Loomis, B. King, T. Burkhead, P. Xu, N. Bessler, E. Terentjev, and B. Panchapakesan, *Nanotechnology* **23**, 045501 (2012).
- ¹²C. Wang, X. Han, P. Xu, X. Zhang, Y. Du, S. Hu, J. Wang, and X. Wang, *Appl. Phys. Lett.* **98**, 072906 (2011); S. A. Mikhailov and K. Ziegler, *Phys. Rev. Lett.* **99**, 016803 (2007); V. P. Gusynin, S. G. Sharapov, and J. P. Carbotte, *ibid.* **98**, 157402 (2007); L. Ju, B. Geng, J. Horng, C. Girit, M. Martin, Z. Hao, H. A. Bechtel, X. Liang, A. Zettl, Y. R. Shen, and F. Wang, *Nanotechnology* **6**, 630 (2011).
- ¹³Y. Zhu, S. Murali, M. D. Stoller, K. J. Ganesh, W. Cai, P. J. Ferreira, A. Pirkle, R. M. Wallace, K. A. Cychoz, M. Thommes, D. Su, E. A. Stach, and R. S. Ruoff, *Science* **332**, 1537 (2011).
- ¹⁴K. S. Kim, Y. Zhao, H. Jang, S. Y. Lee, J. M. Kim, J. H. Ahn, P. Kim, J. Y. Choi, and B. H. Hong, *Nature (London)* **457**, 706 (2009).
- ¹⁵B. Yuan, L. Yu, L. Sheng, K. An, and X. Zhao, *J. Phys. D* **45**, 235108 (2012).
- ¹⁶P. Fan, L. Wang, J. Yang, F. Chen, and M. Zhong, *Nanotechnology* **23**, 365702 (2012).
- ¹⁷B. Lundberg and B. Sundqvist, *J. Appl. Phys.* **60**, 1074 (1986); G. Ausanio, C. L. Hison, V. Iannotti, L. Lanotte, and L. Lanotte, *ibid.* **110**, 063903 (2011); S. Leleu, H. Abou-Kandil, and Y. Bonnassieux, *IEEE Trans. Instrum. Meas.* **50**, 1577 (2001); H. Rajoria and N. Jalili, *Compos. Sci. Technol.* **65**, 2079 (2005); S. Tian and X. Wang, *J. Mater. Sci.* **43**, 4979 (2008); S. Tian, F. Cui, and X. Wang, *Mater. Lett.* **62**, 3859 (2008); T. Furukawa, M. Date, E. Fukada, and Y. Tajitsu, *Jpn. J. Appl. Phys., Part 2* **19**, L109 (1980); F. Fang, W. Yang, M. Z. Zhang, and Z. Wang, *Compos. Sci. Technol.* **69**, 602 (2009); W. K. Sakamoto, P. Marin-Franch, and D. K. Das-Gupta, *Sens. Actuators, A* **100**, 165 (2002); X. F. Liu, C. X. Xiong, H. J. Sun, L. J. Dong, R. Li, and Y. Liu, *Mater. Sci. Eng., B* **127**, 261 (2006); G. Rujijanagul, S. Jompruan, and A. Chaipanich, *Curr. Appl. Phys.* **8**, 359 (2008); A. Chaipanich, N. Jaitanong, and R. Yimnirun, *Ceram. Int.* **37**, 1181 (2011).
- ¹⁸C. Brosseau and P. Talbot, *Meas. Sci. Technol.* **16**, 1823 (2005); A. Mdarhri, C. Brosseau, and F. Carmona, *J. Appl. Phys.* **101**, 084111 (2007); C. Brosseau, A. Mdarhri, and A. Vidal, *ibid.* **104**, 074105 (2008); C. Brosseau, W. Ndong, V. Castel, J. Ben Youssef, and A. Vidal, *ibid.* **102**, 024907 (2007); C. Brosseau, A. Mdarhri, and W. Ndong, *ibid.* **104**, 074907 (2008); A. Mdarhri, P. Elies, and C. Brosseau, *ibid.* **104**, 123518 (2008); M. E. Achour, C. Brosseau, and F. Carmona, *ibid.* **103**, 094103

- (2008); C. Brosseau and M. E. Achour, *ibid.* **105**, 124102 (2009); S. El Bouazzaoui, A. Droussi, M. E. Achour, and C. Brosseau, *ibid.* **106**, 104107 (2009).
- ¹⁹I. Alig, D. Lellinger, S. M. Dudkin, and P. Pötschke, *Polymer* **48**, 1020 (2007); I. Alig, T. Skipa, M. Engel, D. Lellinger, S. Pegel, and P. Pötschke, *Phys. Status Solidi B* **244**, 4223 (2007); I. Alig, D. Lellinger, M. Engel, T. Skipa, and P. Pötschke, *Polymer* **49**, 1902 (2008); I. Alig, T. Skipa, D. Lellinger, and P. Pötschke, *ibid.* **49**, 3524 (2008).
- ²⁰L. Xian, S. B. Lopez, and M. Y. Chou, *Phys. Rev. B* **84**, 075425 (2011).
- ²¹J. J. Liang, Y. Wang, Y. Huang, Y. F. Ma, Z. F. Liu, J. M. Cai, C. D. Zhang, H. J. Gao, and Y. S. Chen, *Carbon* **47**, 922 (2009); S. De and J. N. Coleman, *ACS Nano* **4**, 2713 (2010).
- ²²X. Liu, Y. Wu, X. Wang, R. Li, and Z. Zhang, *J. Phys. D* **44**, 115402 (2011); A. Mejdoubi and C. Brosseau, *Phys. Rev. B* **74**, 165424 (2006); A. Mejdoubi and C. Brosseau, *J. Appl. Phys.* **102**, 094104 (2007).
- ²³O. V. Yazyev and L. Helm, *Phys. Rev. B* **75**, 125408 (2007); D. W. Boukhvalov, M. I. Katsnelson, and A. Lichtenstein, *ibid.* **77**, 035427 (2008); J. Zhou, Q. Wang, Q. Sun, X. S. Chen, Y. Kawazoe, and P. Jena, *Nano Lett.* **9**, 3867 (2009); R. Nair, M. Sepioni, I.-L. Tsai, O. Lehtinen, J. Keinonen, A. V. Krasheninnikov, T. Thomson, A. K. Geim, and I. V. Grigorieva, *Nat. Phys.* **8**, 199 (2012).
- ²⁴J. Du and H.-M. Cheng, *Macromol. Chem. Phys.* **213**, 1060 (2012).
- ²⁵F. T. Fisher, R. D. Bradshaw, and L. C. Brinson, *Appl. Phys. Lett.* **80**, 4647 (2002); K. Wakabayashi, C. Pierre, D. A. Dikin, R. S. Ruoff, T. Ramanathan, L. C. Brinson, and J. M. Torkelson, *Macromolecules* **41**, 1905 (2008); M. A. Rafiee, J. Rafiee, I. Srivastava, Z. Wang, H. Song, Z.-Z. Yu, and N. Koratkar, *Small* **6**, 179 (2010); T. Kuilla, S. Bhadra, D. Yao, N. H. Kim, S. Bose, and J. H. Lee, *Prog. Polym. Sci.* **3**, 1350 (2010); R. Sengupta, M. Bhattacharya, S. Bandyopadhyay, and A. K. Bhowmick, *ibid.* **36**, 638 (2011).
- ²⁶G. M. Odegard, T. C. Clancy, and T. S. Gates, *Polymer* **46**, 553 (2005).